Journal of NUCLEAR SCIENCE and TECHNOLOGY, Supplement 3, p. 49–55 (November 2002)

5f Localization in Ultrathin Pu Layers

Thomas GOUDER,[1,*] Ladislav HAVELA,[1,2] Franck WASTIN,[1] Jean REBIZANT[1]

[1] European Commission, Joint Research Centre, Institute for Transuranium Elements, Postfach 2340, D-76125 Karlsruhe, Germany
[2] Department of Electronic Structures, Charles University, Ke Karlovu 5, 121 16 Prague 2, The Czech Republic

The deposition of Pu on Mg substrate allowed to prepare pure Pu layers with controlled thickness down to 1 monoatomic layer, only weakly interacting with the substrate. High-resolution UPS and Pu-*4f* core-level spectra demonstrate the dramatic changes of electronic structure for Pu below 5 monolayers thickness. For the „thick" layer one can see the spectral intensity representing a *5f* band, increasing up to the Fermi level cut-off. The reduced thickness leads to a new feature around 1.7 eV below E_F. This broad maximum is of *5f* origin, and corresponds roughly to the *5f* emission found in PuSb. Therefore we interpret it as due to the emission from *5f* states, which get localized due to the reduced Pu coordination number. Another set of experiments reveals how the electronic structure of Pu is sensitive to details of crystal structure at the surface. The valence band spectra of α-Pu, prepared by ion-etching at various temperatures, show a systematic development from the triangular form, characteristic for low-*T* surface preparation, into the δ-Pu type, with 3 peaks close to E_F, obtained at elevated temperatures. This supports the theoretical conjecture that the surface of α-Pu should have a δ-Pu character.

KEYWORDS: ***Pu, photoelectron sprectroscopy***

I. Introduction

It has been generally accepted that high-resolution valence-band photoelectron spectra of actinide metals[1] exhibit a gradually increasing *5f* spectral intensity in the sequence Th, U, Np, Pu. It is broad, has no distinct sharp features, reaches maximum at the Fermi energy E_F, and indicates the itinerant character of the *5f* states. The *5f* localisation in Am leads to a shift of the *5f* emission from the Fermi level and appearance of a multiplet structure. Photoelectron spectroscopy proved thus to be a very convenient tool to distinguish between the band and localized situations.

Being right at the localisation threshold, Pu has an especially interesting position within the actinide series showing large volume variations between the allotropic phases[2)]. The loss of the *5f* bonding means a loss of a part of the cohesive energy and leads to the higher atomic volume. At the same time, the system gains some energy (coming from Coulomb and spin-orbit interactions) by more correlated motion of electrons in atomic-like *5f* states. Seen from the other side, the volume variations are strongly affecting the overlap of the *5f* wave functions centered on neighbouring Pu ions; the larger overlap increases the width of the *5f* band, or, more generally, tends to a more delocalized character of the *5f* states.

The low-temperature phase α-Pu (monoclinic) can be described as a *5f*-band system, albeit with strong electron-electron correlations. The other most prominent phase is δ-Pu, stable between 592 and 724 K, which has the largest volume (by 20% larger than the α-phase). As it can be stabilised in a larger temperature range by doping, low-temperature data are also available[3]. The weakly magnetic character of α- and δ-Pu are similar, but LDA calculations of δ-Pu assuming *5f*-itinerancy have difficulty in accounting for the cohesion properties[4,5)]. New theoretical approaches, emerging recently to account for δ-Pu properties, assume that part of the *5f* states are localised, whereas the itinerancy is still preserved for the remaining states[4)], or span the Mott transition using a dynamical mean-field theory[6)].

The rather simple picture of featureless spectra of the *5f* band mentioned above was obtained for the α-Pu phase[1]. The valence-band spectra of the δ-phase exhibit a Fermi-level peak narrower than for α-Pu, and there is another distinct maximum at 0.8 eV binding energy[7)]. The dramatic difference between the valence-band spectra of α- and δ-Pu was not confirmed by later experiments[8)]. In that work, the δ-Pu features shown in Ref. 7 are reproduced, but α-Pu is strikingly similar to that, also displaying another maximum at

---

[*] phone: ++49-7247-951243, fax: ++49-7247-951587, e-mail: gouder@itu.fzk.de

0.8 eV, which is only somewhat weaker than for δ-Pu.

In this work we study the impact of varying degree of the 5f localization on photoemission spectra. In the first part we compare α-Pu with surface prepared under various conditions, which provides information about where differences in α-Pu spectra may originate, with δ-Pu. In the second part we demonstrate how the development of localization can be extended for ultrathin Pu films, reaching the limit for one monolayer. The UPS valence-band spectra are complemented by the *4f*-core level spectra. Generally, we could identify three types of features, belonging to the localized *5f* states, to band *5f* states, and a group of features appearing at an intermediate delocalization.

II. Experimental

The work described was performed in a photoelectron spectrometer equipped with Leybold LHS 10 hemispherical analyzer; which is placed in a glove box dedicated to transuranium materials. XPS spectra were taken using the Al-K_α (1486.6 eV) radiation. The energy resolution (combined line width and instrumental resolution) is about 1.0 eV. UPS studies were done using HeI and HeII (21.22 and 40.81 eV) excitation radiation, produced by a windowless UV discharge source. The resolution in UPS was 45 meV for most experiments. The *5f* photoexcitation cross section is dominating for HeII radiation, whereas it is very weak for HeI, and thus differences help to identify the emission of the *5f* origin. Furthermore, the relatively high cross section of O-*2p* states for HeII excitation makes the HeII spectra very sensitive indicator of any O contamination, far superior to the standard monitoring of the O-*1s* line in XPS.

Measurements were performed partly on bulk samples of α-Pu, purified by long-term heating while sputtering the surface by Ar ions. As it is practically impossible to avoid a slow subsequent surface contamination even if the sample is cooled to T = 77 K, the surface has to be studied within several minutes after the sputtering. This time is progressively reduced at higher temperatures, and studies of clean surface at temperatures above the room temperature are difficult. On the other hand, thin layers yield the possibility of clean surfaces stable even at elevated temperatures, as the reservoir of impurities below the surface is eliminated. To use this possibility, we have constructed a DC sputter source attached to the preparation chamber of the spectrometer. Low Ar gas pressure (10^{-3} torr) minimizes the contamination of sputtered material by gas impurities. Stabilization of plasma at low working pressures is achieved by injecting electrons of about 100 eV energy from a hot W filament. The target, which can be smaller than 100 mg of material, is kept at room temperature, the substrate can be cooled down to T = 77 K, or heated up to several hundred °C. The deposition rate is typically 0.1 monolayer per second. The target for sputtering was pure α-Pu.

III. Valence band spectra of α-Pu

Photoemission on α-Pu was studied already by several groups[1,8)]. Unfortunately, the data reveal a considerable discrepancy. The broad triangular emission presented in the first work was obtained for surface prepared by sputtering by Ar ions at T = 77 K. In the latter work, yielding spectra more similar to δ-Pu, authors were using laser ablation.

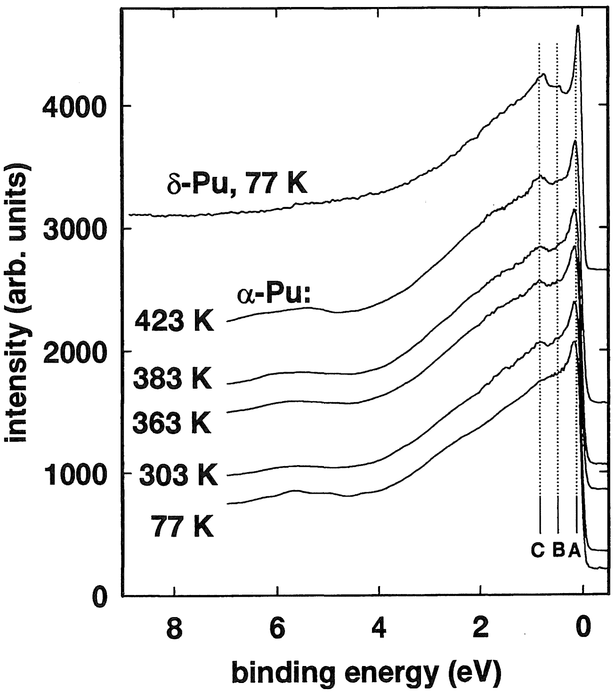

Fig.1: Valence band spectra of bulk α-Pu for the photon energy hν = 40.8 eV, recorded after ion etching at various temperatures indicated in the figure. For comparison, we give the spectrum of δ-Pu recorded at T = 77 K using the same equipment (from Ref. 7). The dotted lines indicate the position of the peaks A, B, and C described below.

To test the influence of preparation temperature, we performed a series of experiments with Ar sputtering of the surface. The results, together with original data[7)] on δ-Pu, are displayed in **Fig.1**. For low temperature surface preparation, our results reproduce very well the results of Ref. 1. For T above the room temperature, the transition towards the δ-Pu character proceeds smoothly, and is seen as the development from a weak satellite at about 0.9 eV (peak C) forming a gap around 0.3 eV. The temperature range could not be extended to higher temperatures, as the surface segregation of oxygen, manifest in the O-$2p$ emission around 6 eV, became severe. Close inspection of α-Pu spectra shows that for this phase the intensity of the three peak structure (well noticeable at the peak C, as the peak A is affected by the broadening due to the Fermi-Dirac statistics, and peak B is rather weak) differs greatly depending on the preparation of the surface, which can explain the discrepancies between Ref. 1) and 8) mentioned above. Surfaces cleaned by laser ablation at low temperature[8)] showed an intense peak C, up to the point that α- and δ-Pu data look similar, whereas surfaces cleaned by sputtering (ion-etching) showed the peak C much weaker.

The conclusion is that the sample temperature during sputter cleaning plays a crucial role. Ion-etching at room or elevated temperatures leads to the growth of peak C. Obviously peak C appears under conditions, in which thermally activated processes lead to a surface reconstruction. Although we did not perform a systematic study of an effect of annealing after a low-temperature surface preparation, there is evidence that relatively fast changes (noticeable on the timescale of minutes) towards the δ-Pu type occur for α-Pu surface even in the temperature range below the room temperature. These changes are also noticeable on the Pu-$4f$ core-level spectra.

These facts corroborate the conjecture introduced in Ref. 9), that the surface of α-Pu can have a different character with more localized $5f$ states, which was also theoretically documented[10)], as the decreased coordination could be a driving force for formation of a non-α phase at the α–Pu surface. In such situation a laser pulse used to remove the upper layers in Ref. 8 could bring thermal energy needed for the reconstruction. On the other hand, the low temperature ion etching removes atoms locally, with a smaller energy flux to the overall surface, which can be less favourable for the reconstruction. Even if the low-T ion etching results in high concentration of defects, these surfaces are closer to the bulk situation for α-Pu than if surface reconstruction occurs as a result of thermally assisted processes.

An alternative explanation would be that the spectra of α-Pu are indeed similar to δ-Pu, and that the Ar ion sputtering at low temperatures leads to an amorphous surface, which then loses the characteristic α-Pu features. To our view, this situation is less plausible as the amorphous surface with larger mean Pu-Pu spacing than in α-Pu would tend to reduce the $5f$ itinerancy. What we observe is probably just opposite, as the broad featureless triangular emission seems to be corresponding to the $5f$ itinerant limit (based on analogy with similarly looking spectra of U and Np).

IV. Ultrathin Pu layers on Mg

Polycrystalline Mg was used as a substrate for this set of experiments. The main reason to use Mg came from our experience with U metal, which does not mix with Mg within the sputter deposition process[11)], unlike e.g the Pu-Al system studied earlier[12)] leading to intermixing and/or reaction of the two components. Prior to deposition, Mg was cleaned by Ar ion sputtering at $T = 150$ °C.

For thick layers, i.e. those for which thickness exceeds substantially the attenuation length, we obtained two somewhat different types of valence-band spectra, depending on the synthesis temperature. For room temperature and lower, the spectra are strongly reminiscent of those of δ-Pu seen in Fig.1, and there is practically no dependence on the deposition temperature (spectrum *a* in **Fig.2**). Spectra are very slightly modified, if the deposited layers are subsequently exposed to sputtering by Ar ion (*b* in Fig.2). This treatment enhances somewhat the emission close to E_F relatively to the peak C, but not to the extent seen for the α-Pu bulk exposed to the same treatment. This finding is indicative of the fact that the Pu thin layers deposited by sputter deposition have more δ-Pu like character, i.e. no genuine α-Pu can be uncovered by the ion etching. Photoelectron spectroscopy cannot naturally answer the question whether we deal with real δ-Pu structure, or simply with a strongly defected structure having similar degree of the $5f$ localization as the δ-Pu.

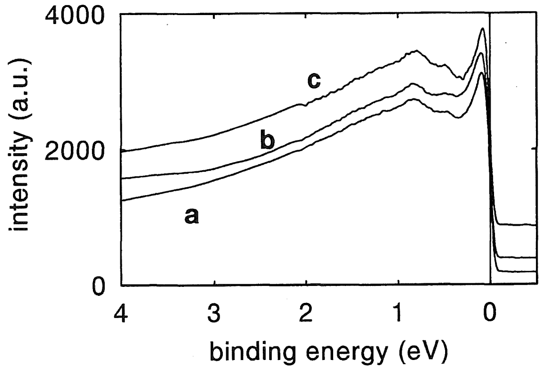

Fig.2: Valence-band spectra of thick Pu layers on Mg for the photon energy hν = 40.8 eV. Spectrum *a* was obtained on a layer deposited at room temperature and studied at $T = 77$ K, spectra for layers deposited at 93 K are practically identical. Spectrum *b* was obtained on the same layer as spectrum *a* after a subsequent ion etching at $T = 77$ K. The spectrum *c* was obtained on the layer deposited at $T = 373$ K, cooled afterwards to $T = 77$ K.

For higher temperatures ($T = 100$ °C and 150 °C), the HeII spectra (spectrum ***c*** in Fig.2) differ in the energy range down to 0.5 eV, where the intensity is somewhat suppressed comparing to the peak C.

As to the situation at the Fermi level, Ref. 8 points out an interesting difference between δ- and α-Pu. In δ-Pu, the peak A is narrower and just at the E_F (within the experimental resolution), whereas for α-Pu it is broader and shifted somewhat below the Fermi level. In our study, we found that the spectra of Pu layers deposited at low T and treated by ion etching (spectrum ***b*** in Fig.2) exhibit the same binding energy as in α-Pu in Ref.8 for the maximum of peak A (100 meV below E_F). The full width at half maximum (FWHM) of the peak is 140 meV. On the other hand, deposition at elevated temperatures ($T > 373$ K) leads to a somewhat different shape of the valence-band spectra (see **Fig.3**), which is reminiscent of that obtained on δ-Pu[8]. The maximum of the peak A appears much closer to the Fermi level (75 meV below E_F) and the peak is sharper (FWHM = 120 meV). Comparison with data taken with higher resolution ($\Delta = 30$ meV), which yield the maximum at 60 meV and FWHM = 110 meV, shows that the peak A is actually located at E_F. The situation for the low temperature deposition without the ion etching (spectrum ***a*** in Fig.2) is intermediate between these two cases.

Even larger shift of the peak A from E_F was found for the bulk α-Pu ion etched at $T = 77$ K. Detailed view of the lowest spectrum in Fig,1 shows that the maximum is much broader, shifted to 160-170 meV below E_F. The fact that at zero energy the intensity is much lower than 50% of the peak maximum points to the situation, in which the Fermi level is located on the descending slope of the density of states, $N(E)$. Comparing other spectra from Fig.1, we observe that increasing temperature of ion etching moves gradually the maximum of the peak A towards E_F. The quantitative analysis is though obscured by the Fermi-Dirac broadening, as the spectra were taken at the temperature identical as the ion-etching temperature.

The gradual variations of the position and width of the peak A lead us to a conjecture, that what is observed experimentally is a superposition of two types of spectra, namely the α-Pu and δ-Pu like from Fig.1, with the weight depending on structural details. In most of cases we can assume that the δ-Pu character is restricted to the surface.

As the sputter deposition of Pu on Mg leaves the interface rather sharp on the atomic scale, without noticeable intermixing, it is possible to prepare ultrathin Pu layers, which have the attenuation length smaller than the actual thickness, and study the effect of reduced dimensionality on the $5f$-localization. The analysis of attenuation of different Mg spectral lines can yield not only the information on the thickness of the Pu overlayer, but provides also an estimate which portion of the surface is left uncovered. Examining the growth modes at various temperatures, we observed that the deposition at ambient and elevated temperatures leads in the early stage to the formation of thicker Pu islands, leaving part of the Mg surface uncovered. When cooling down to about 120 K, the surface is covered in a more uniform way by ultrathin layer, and the thickness can be controlled down to 1 monolayer. Because there is no surface diagnostics as STM or LEED available, we do not know details of the surface morphology. The nominal thickness values indicated have to be therefore taken as average, effective values.

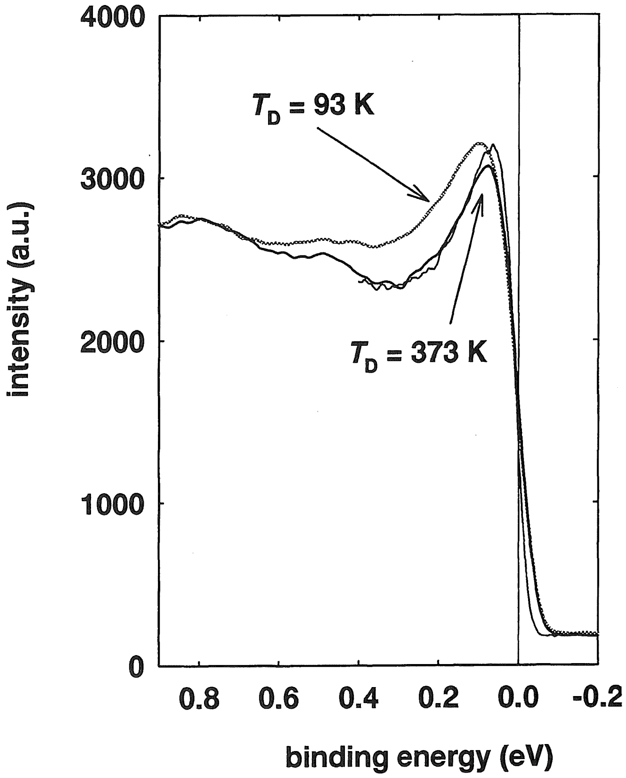

Fig.3: Detail of the valence-band spectra of thick Pu layer showing the difference in the position of the peak A. The layers were deposited at $T_D = 93$ K and 373 K, respectively, the spectra were taken at $T = 77$ K in both cases. The thin line for $T_D = 373$ K represents the spectrum taken with higher resolution ($\Delta = 30$ meV).

HeII spectra of Pu ultrathin layers demonstrate that the $5f$-localization can be varied in a much larger extent when approaching the limit of dimension 2. **Fig. 4** shows essentially not 3, but 4 distinct spectral features in the Pu valence band. At low coverage (1 ML Pu) the spectrum is dominated by a relatively broad asymmetrical peak (D) centred at 1.6 eV BE. On its low binding energy side, 3 weak peaks appear, at 0.85 eV (C), 0.50 eV (B), and at (or in the close vicinity of) E_F (A), which can be identified with features observed in the δ-Pu spectra[7].

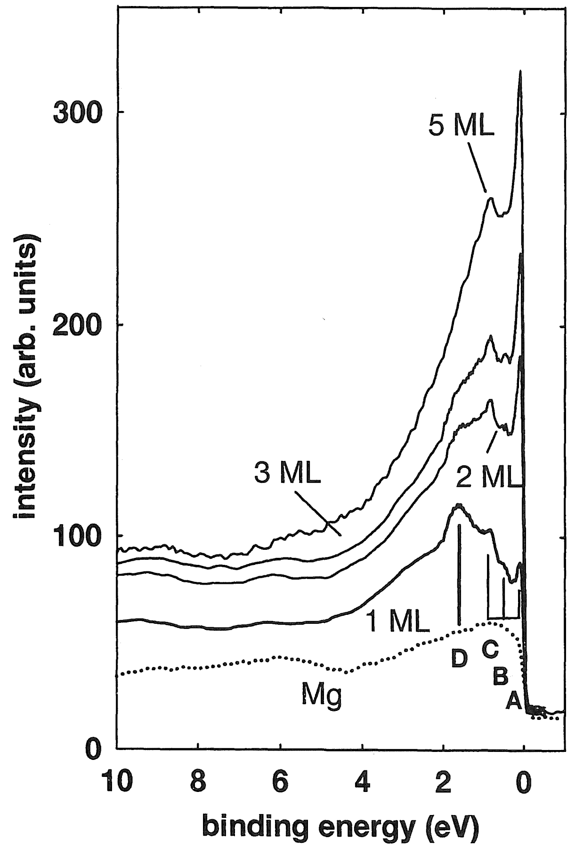

Fig.4: Valence-band spectra of pure Mg substrate and increasing coverage of Pu. The thickness is indicated in number of monolayers (ML). Spectra obtained with the photon energy $h\nu = 40.8$ eV. The vertical bars indicate the position of the *5f*-localized peak and the triplet of narrow features, described in the text.

With increasing Pu coverage, the peak D is gradually suppressed, and majority of the spectral weight is transferred into the range from 0 to 1 eV. The three sharp features A, B, and C increase in intensity, and we can also deduce that a background *5f* density of states of roughly triangular shape, gradually increasing from about 1 eV up to E_F, is growing below the 3 peaks, the energy positions of which do not change. We may attribute this triangular emission to *5f* band states, as we assume that this is the dominant contribution for α-Pu, as displayed in Fig.1. The peak D is similar in energy and shape to features observed in PuSe and PuSb, which are due to localized *5f* states[13], which probably form a multiplet similar to Am, but individual components remain unresolved.

Comparison of the HeII with those obtained for the HeI radiation (not shown here) proves that the peak D is of the *5f* origin. The *5f*-photoexcitation cross section in HeI radiation is negligible[1], and the peak D is indeed vanished in the HeI spectra. Therefore we can interpret the peak D as due to the localized *5f* states, which do not hybridize with other electronic states. For the thickness of 2 monolayers (thick layers behave in analogous way), this not fully true for the peaks C, B, and especially A, which remains clearly most emphasized. This means that the peak A shows an appreciable admixture of *6d* states (which normally form a rather broad band), as the *7s* photoexcitation cross section is very weak. In another words, it points to a significant *5f-6d* hybridization effects imprinting the pronounced feature of the *5f* density of states onto the *6d* states in the Fermi level vicinity. The enhancement of the Fermi level emission in HeI was not observed for the 1 ML case. This fact can be understood as the *5f* localization suppresses the hybridization of the residual *5f*-states at E_F with the *6d* states.

Besides the different cross section, the difference can generally arise due to different attenuation length, which is about 1.0 nm for HeI but only 0.5 nm for HeII. Due to that, HeI spectra normally carry more information about the sub-surface area than the HeII spectra, which are even more surface-sensitive. But the case of the 2 ML thick Pu layer, at which the attenuation effects must remain secondary, demonstrates that the *5f-6d* hybridization must be taken responsible at least for a part of this effect.

The main conclusion that the *5f* localization has been observed with decreasing thickness of Pu layers. At first glance, we can reproduce the spectra of δ-Pu by reducing the nominal layer thickness from 5 to 2-3 monolayers. Reducing even further the layer thickness results in the appearance of the *5f* localised peak. The localization of the *5f* states can be understood as due to the reduced dimensionality, reducing the effective number of nearest neighbour atoms, which favourise the situation in which the *5f* states do not participate to bonding.

V. Pu-*4f* core-level spectra

The Pu-*4f* core-level spectra consist of two distinct peaks, $4f_{5/2}$ and $4f_{7/2}$, split by s-o interaction. For both α–and δ-Pu each of the peaks consists of two features. According to the two screening channel model[14], the final-state *4f* hole can be screened by the Coulomb interaction attracting to it a *5f*-electron (so called good screening). But in a case if the probability of such process is low, a more excited final state related to a non-*f* (so called poor) screening dominates . The first channel gives rise to a narrow spectral line, the asymmetry of which is due to additional energy losses while creating electron-hole pairs at the Fermi level by a photoexcited electron.

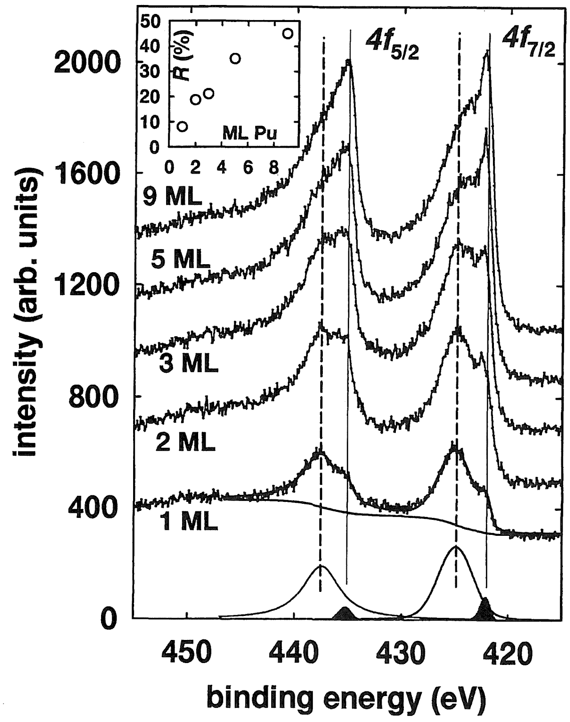

Fig.5: Pu-*4f* spectra for increasing Pu layer thickness (given in monolayers ML). The position of well-screened features is indicated by the full vertical lines, that of the poorly screened features by the dashed lines. For the 1 ML spectrum we display also the background and the fit, with individual components at the baseline (the poorly screened components as empty peaks, the well screened components as full peaks). The inset shows the variation of the intensity ratio R of the well screened and poorly-screened $4f_{5/2}$ components as a function of Pu layer thickness.

The second spectral feature is broader, involving an unresolved manifold of states due to the *4f* hole interacting with different states of the multiplet of the localized *5f* states. In Pu systems studied, the smaller width of the $4f_{7/2}$ poorly-screened peak gives better chance to distinguish the two channels than for the broader $4f_{5/2}$ peak. For α-Pu, the narrow, so called well screened, feature at lower binding energies dominates[1]. For δ-Pu the intensity of the poorly screened feature is appreciably stronger[15]. The relative intensity need not be directly proportional to the degree of localization in the ground state, as it is pertinent to the strongly perturbed final state (different potential, lack of periodicity). But it is reasonable to assume that the development of the *5f* localization is qualitatively related with the growth of the poorly screened features. **Fig.5** shows the development of the *4f* spectra for ultrathin Pu layers, which correspond to valence-band spectra shown in Fig.4.

The well screened feature, which is barely noticeable for 1 ML Pu, for which the final state with localized *5f* electronic states dominates, increases with increasing thickness, reaching saturation at about 10 ML, and we obtain the *4f* spectra typical for bulk Pu[1] at such coverages already.

To quantify the spectra variations, we fitted the spectra (after integral background subtraction) using Gamma functions accounting for the asymmetry in case of the two well screened features, whereas the poorly screened features were approximated by Voigt functions. We did not use any particular microscopic model, as the spectra in fact demonstrate a cross over from the clear *5f*-band situation in α-Pu to localized Pu in 1 ML case, and no simple model can cover all regimes in between. The two features are better resolved for the $4f_{7/2}$ peak, therefore we use this peak to compare relative intensities of the two features. Whereas for 1 ML the intensity of the well screened feature is only 7% of the poorly screened one, this value increases and reaches 45 % for 9 ML. (See the inset in Fig.5.) One should be aware that the attenuation length is larger for the electrons ejected by X-rays from the *4f* states (approx. 1.5 nm) than for the valence-band electrons excited by UV radiation. Consequently, the *4f* spectra can carry information from a deeper sub-surface area, whereas HeI and especially HeII valence-band spectra are more surface sensitive. This fact can play a certain role for more massive layers.

The binding energies (BE) of the well screened features are identical to those found in bulk α-Pu (422.2 eV and 435.1 eV for $4f_{5/2}$ and $4f_{7/2}$, respectively), whereas the poorly screened peaks are centred at energies about 2.4 eV higher. Comparing the large intensity variations related to the layer thickness (from dominating well-screened to dominating poorly-screened features), the difference of α- and δ-Pu is rather moderate, suggesting that in δ-Pu the *5f* states, or at least large portion of them, are still itinerant.

As mentioned above, the intensity of poorly screened peaks can lead to an overestimation of the *5f* localization due to the presence of the *4f* hole. On the other hand, the type of the *4f* spectrum for 1 ML is already very close to that of PuSb[12], which can be taken as a Pu archetype with localized *5f* states. Having in mind that the Pu coverages are nominal, i.e. some inhomogeneity in coverage persists, we may consider the small residual spectral intensity in the well screened features as being due to a small number of somewhat thicker Pu clusters. Comparison with valence band data allows us to exclude any influence of a surface Pu oxide, which normally yields poorly screened features in the *4f* spectrum.

VI. Discussion and conclusions

We can summarize that all Pu phases display in general three different types of spectral features: the signal of well delocalised *5f* states (broad triangular peak with maximum at E_F), the three-peak structure (most prominent in δ-Pu), and the peak around 2 eV BE characteristic of the localized *5f* states. The three sharp peaks typical for intermediate delocalization appear always together, at energies identical for all systems studied, although the intensity varies. We can therefore assume a common mechanism for all three in all the cases. Earlier we observed features at the same energies in PuSe [13] (both bulk and thin layers) and also for a Pu-Si. They are not observed in *5f* localized PuSb [13] and tend to vanish in the thin-layer Pu limit.

As yet, these features have not been reproduced in electronic structure calculations, and in fact their general occurrence is a clear signal that they are not related to the band structure of any particular material. Consequently, they cannot be explained within one-electron picture. We can thus think of two possible types of origin of these features. Assuming the localized *5f* peak at 1.6 eV as analogous to the *5f* emission in PuSb (which is coming from the $5f^5 \rightarrow 5f^4$ transitions), we can speculate that the features closer to E_F are due to a different multiplet of localized states. In particular, the $5f^6 \rightarrow 5f^5$ transition should appear closer to E_F in this case. This would mean that not only PuSe, but also δ-Pu would be mixed-valence materials, with the *5f* configuration fluctuating between $5f^5$ and $5f^6$. We though feel as more plausible explanation based on many-body phenomena, arising due to the hybridization between localized *5f* and conduction-electron states, which can be taken as an analogy of the Kondo effect, known from Ce-or Yb-based systems. The analogy with the Kondo effect may help to understand the pronounced peak at E_F, which shows a non-negligible non-*f* admixture, as a sort of Kondo resonance, which could account for example for the enhancement of the specific heat γ coefficient in δ-Pu ($\gamma = 53$ mJ/mol K^2) (16.

Acknowledgements. Authors are grateful to G.H. Lander and M.S.S. Brooks for a fruitful discussion. High purity Pu metal was made available through a loan agreement between Lawrence Livermore National Laboratory and Institute for Transuranium Elements in the frame of a collaboration involving Los Alamos National Laboratory and the U.S. Department of Energy.

References

1) J.R.Naegele, L.Manes, J.C.Spirlet, W.Müller, Phys.Rev.Lett., **52**(1986)1834-1837; J.R.Naegele, J.Ghijsen, L.Manes, in: *59/60 Structure and Bonding, Actinides - Chemistry and Physical Properties*, edited by L.Manes (Springer Berlin) 1985, pp. 197-262.

2) J.L.Smith, Z.Fisk, S.S.Hecker, Physica **130B**(1985)151-158; A.C.Lawson, B.Cort, J.A.Roberts, B.I.Bennet, T.O.Brun, R.B.Von Dreele, J.W.Richardson, Jr., In: *Electron Correlations and Materials Properties*, edited by A.Gonis, N.Kioussis, and M.Ciftan, (Kluwer Academic/Plenum, New York) 1999, pp. 75-96.

3) S.Meot-Reymond and J.M.Fournier, J. Alloys Comp., **232**(1996)119-125.

4) O.Eriksson, J.D.Becker, A.V.Balatsky, J.M.Wills, J.Alloys Comp., **287**(1999),1-5; L.Petit, A.Svane, W.M.Temmerman, Z.Szotek, Solid State Commun., **116**(2000)379-383.

5) J. Bouchet, B. Siberchicot, F. Jollet, A. Pasturel, J. Phys.: Condens. Matter **12**, 1723 (2000); S.Y.Savrasov and G.Kotliar, Phys.Rev.Lett., **84**(2000)3670-3673.

6) S.Y. Savrasov, G. Kotliar, E. Abrahams, Nature, **410**(2001)793-1795.

7) J. Naegele, in *Landolt-Börnstein Numerical Data and Functional Relationships in Science and Technology, New Series III/23b*, Springer 1994, p. 183-327.

8) A.J.Arko, J.J.Joyce, L.Morales, J.M.Wills, J.Lashley, F.Wastin, J.Rebizant, Phys.Rev.B, **62**(2000)1773-1779.

9) L.E.Cox, O.Eriksson, B.R.Cooper, Phys.Rev.B, **46** (1992) 13571-13575.

10) O.Eriksson, L.E.Cox, B.R.Cooper, J.M.Wills, G.W.Fernando, Y.G.Hao, A.M.Boring, Phys.Rev.B, **46**, (1992)13576-13583.

11) T.Gouder, Surface Science, **382**(1997)26-34.

12) T.Gouder, J.Electron Spectroscopy and Related Phenomena **101-103**(1999) 419-422.

13) T.Gouder, F.Wastin, J.Rebizant, L.Havela, Phys.Rev.Lett. **84**(2000)3378-3380.

14) J.C.Fuggle, M.Campagna, Z.Zolnierek, R.Lässer, A.Platau, Phys.Rev.Lett., **45**(1980)1597-1600.

15) L.E. Cox, Phys.Rev.B, 37(1988)8480-8483.

16) G.R.Stewart and R.O.Elliott, in Absrtracts for Actinides 1981, LBLRep., LBL-12441, 1981, Lawrence Berkeley National Laboratory, CA, p.206.